


Article

Evaluation for Simultaneous Removal of Anionic and Cationic Dyes onto Maple Leaf-Derived Biochar Using Response Surface Methodology

Yong-Keun Choi ^{1,2} , Ranjit Gurav ¹, Hyung Joo Kim ^{1,2}, Yung-Hun Yang ^{1,3}
and Shashi Kant Bhatia ^{1,3,*}

¹ Department of Biological Engineering, Konkuk University, Seoul 05029, Korea; dragonrt@konkuk.ac.kr (Y.-K.C.); rnjgurav@gmail.com (R.G.); hyungkim@konkuk.ac.kr (H.J.K.); seokor@konkuk.ac.kr (Y.-H.Y.)

² The Academy of Applied Science and Technology, Konkuk University, Seoul 05029, Korea

³ Institute for Ubiquitous Information Technology and Applications (CBRU), Konkuk University, Seoul 05029, Korea

* Correspondence: shashikonkukuni@konkuk.ac.kr; Tel.: +82-2-3437-8360

Received: 24 March 2020; Accepted: 21 April 2020; Published: 25 April 2020



Abstract: Rapid development in the printing and dying industry produces large amounts of wastewater, and its discharge in the environment causes pollution. Keeping in view the carcinogenic and mutagenic properties of various dyes, it is important to treat dyed wastewater. Maple leaf biochars were produced at different pyrolysis temperatures, i.e., 350 °C, 550 °C, and 750 °C, characterized for physicochemical properties and used for the removal of cationic (methylene blue (MB)) and anionic dye (congo red (CR)). Response surface methodology (RSM) using three variables, i.e., pH (4, 7, and 10), pyrolysis temperature (350 °C, 550 °C, and 750 °C), and adsorption temperature (20 °C, 30 °C, and 40 °C), was designed to find the optimum condition for dyes removal. X-ray diffraction (XRD) analysis showed an increase in CaCO₃ crystallinity and a decrease in MgCO₃ crystallinity with the increase of pyrolysis temperature. RSM design results showed that maple biochar showed maximum adsorption capacity for cationic dye at higher pH (9–10) and for anionic dye at pH 4–6, respectively. Under the selected condition of pH 7 and an adsorption temperature of 30 °C, biochar MB550 was able to remove MB and CR by 68% and 74%, respectively, from dye mixtures. Fourier transform infrared (FTIR) and X-ray photoelectron spectroscopy (XPS) analyses showed that MB550 was able to remove both dyes simultaneously from the aqueous mixtures.

Keywords: biochar; methylene blue; congo red; response surface methodology; maple leaf

1. Introduction

Dyes are widely used in various industries, such as textiles, plastics, paper, and leather production [1,2]. The large amounts of dye effluents occurred from these factories can infiltrate (approximately 85%) and accumulate into ground water and surface water systems [3]. These dye effluents, by transferring into drinking water, have caused significant problems, such as a threat of human health owing to mutagenic, carcinogenic, and toxic characteristics of dyes [1,2]. Therefore, it is necessary to evaluate and investigation methods to eliminate dyes from aqueous environment.

Technologies including physical, chemical, and biological processes for dye removal have been studied [1,4,5]. The chemical process has its own problems, such as the production of harmful intermediates and a high cost of operation [6]. In addition, the biological process has a disadvantage including the limits for removal efficiency due to a synthetic origin and stable molecular structure of dye, occurrence of sludge, and production of secondary harmful compounds [1,3]. Currently, the physical

processes, including activated carbon, ion exchange, and membrane filter, appear attractive because of their high performance, and facile reaction process [4]. However, these physical processes also possess limits, such as high cost of material and equipment [7].

As a promising adsorption-based approach, biochars (BCs) can be effectively used for dye treatment. BCs produced from waste bioresource residues, such as wood, leaves, sawdust, weeds, straws, and microalgae, are inexpensive and chemically and mechanically stable adsorbents [8–10]. BCs can be easily modified using various approaches, such as surface oxygenation and preparing their composites with other materials, to increase the adsorption efficiency [11–13]. In particular, the pyrolysis temperature is one of the crucial parameters for biochar production and may affect its characteristics with regard to dye treatment. According to the previous literature, BCs produced at different pyrolysis temperatures possessed different properties (e.g., metal crystallization, functional groups, surface area, pH_{pzc} (the pH at point of zero charge), and porous structure) [2,10,14,15]. Hence, seaweed-, vermicompost-, cabbage-, wheat straw-, pulp-, and paper sludge-derived BCs from previous studies were used for dye removal (e.g., methylene blue, congo red, crystal violet, etc.) [2,4,8,16,17]. Yang et al. (2016) reported that there were possible mechanisms such as hydrogen bond formation, π - π interaction, electrostatic attraction, and cation exchange for MB and CR dye removal using vermicompost-derived BCs [2].

In addition, the adsorption by activated carbons governed a higher surface area and mesoporous nature [4]. There are some difficulties for the treatment of dyes possessing different characteristics (e.g., cationic and anionic property). In particular, characteristics of these dye effluents could be dependent on the production process, season, and era. Therefore, BCs having various characteristics can be advantageous for the simultaneous treatment of dyes mixtures. Thus, this study focused on the adsorptive elimination of cationic and anionic dye mixtures (i.e., methylene blue and congo red) as cationic and anionic dye in water using BCs produced at various pyrolysis temperatures. In order to evaluate the adsorption efficiency of the dye, we tried to investigate the optimal and possible condition using response surface methodology (RSM).

The main objectives of this investigation are to: (1) rapidly evaluate the optimization (i.e., solution pH (4, 7, and 10), pyrolysis temperature (350, 550, and 750 °C), and adsorption temperature (20, 30, and 40 °C)) of the dyes (i.e., methylene blue and congo red) adsorption onto BCs via response surface methodology (RSM), (2) figure out the adsorption mechanisms between dyes and BCs, and (3) examine the adsorption of mixtures of dyes (methylene blue and congo red) onto BCs in optimal condition of batch experiments.

2. Materials and methods

2.1. Chemicals

Methylene blue (hereafter, MB) and congo red (hereafter, CR) used to evaluate adsorption efficiency of BCs were purchased from Sigma-Aldrich Korea. Table 1 shows the characteristics of dyes used in the current investigation [18]. Maple leaves (*Acer palmatum*) collected from Konkuk University campus (Seoul, Korea) were used as feedstock for BCs production.

Table 1. Characteristics of methylene blue and congo red used in the current investigation.

Dye	Empirical Formula	Color Index	Molecular Weight (g/mol)	λ_{\max} (nm)	pKa	Molecular Structure
Methylene blue	C ₁₆ H ₁₈ ClN ₃ S	52015	319.85	670	2.6, 11.2	
Congo red	C ₃₂ H ₂₂ N ₆ Na ₂ O ₆ S ₂	22120	696.66	500	4.1	

2.2. Preparation of BCs

The preparation of maple leaf-derived BCs was described in our previous study [9]. Briefly, the maple leaves were dried at 60 °C overnight and crushed to 500–2360 µm particle size. Maple leaf-derived BCs were produced from feedstock (i.e., maple leaf) using a pyrolysis reactor (Tube Furnace OTF-1200X-S, MTI Co., Richmond, CA, USA). The pyrolysis was conducted after reaching each temperature (350 °C, 550 °C, and 750 °C) with 10 °C/min under nitrogen atmosphere for 2 h. The maple leaf-derived BCs were named corresponding to pyrolysis temperature (i.e., BC350, BC550, and BC750). The maple leaf-derived BCs were ground into powder and sieved to below 106 µm particle size. Ten grams of maple leaf-derived BCs were washed to remove the impurities using 1000 mL of distilled (DI) water several times for 3 days.

2.3. Characterization of BCs

The surface area of BCs was analyzed by using the Brunauer–Emmett–Teller (BET) method, and the area was determined using N₂ adsorption data at 77K (TriStar II, Norcross, Micromeritics, USA). The elemental contents of C, N, and H in feedstock and BCs were determined by a Thermo elemental analyzer (FLASH EA1112, Waltham, Thermo Scientific, USA). The O content was calculated based on the difference of the C, H, N, and ash contents. In addition, O/C and H/C were also calculated by O, H, and C (mol/mol). According to the experimental method in a previous study, the pH at point of zero charge (pH_{pzc}) was measured to determine the surface charge of BCs [19]. XRD (X-ray diffraction) analysis (SmartLab, Rigaku Co., Japan) was conducted by scanning at a range of 2° to 80° with a step size of 0.02° (2θ) to determine the metal crystallization on the surface of BCs. The surface functional groups on BCs were analyzed by Fourier transform infrared (FTIR) spectroscopy (FT/IR-4600, Jasco, Japan) at a wavelength range between 400 and 4000 cm^{−1}. X-ray photoelectron spectroscopy (XPS) analysis (K-Alpha, Waltham, Thermo Scientific, USA) was performed to observe the binding energy of surface compositions on BCs.

2.4. RSM Design and Statistical Analysis

A Box–Behnken design was used for response surface methodology (RSM) analysis and to describe the influences of the various parameters on adsorption efficiency of MB and CR onto BCs. As shown in Table 2, three main factors and levels were chosen: solution pH (X₁), pyrolysis temperature of a produced BCs (°C) (X₂), and dye adsorption temperature (°C) (X₃). The experimental data were analyzed to fit a second-order polynomial model by Equation (1):

$$Y = \beta_0 + \sum_{i=1}^k \beta_i X_i + \sum_{i=1}^k \beta_{ii} X_i^2 + \sum_{i=1}^k \sum_{j=1}^k \beta_{ij} X_i X_j + \varepsilon \quad (1)$$

where Y is adsorption efficiency; β_0 , β_i ($i = 1, 2, 3$), β_{ii} ($i = 1, 2, 3$), and β_{ij} ($i = 1, 2, 3; j = 1, 2, 3$) are the various coefficients, while X_i and X_j are coded independent variables. The Minitab 16 Statistical software was used to analyze the data.

Table 2. Coded and actual values of the various variables (pH, pyrolysis, and adsorption temperature) used in Box–Behnken design.

Factor	Variables	Levels of Variables		
		−1	0	+1
X1	Solution pH	4	7	10
X2	Pyrolysis temperature (°C)	350	550	750
X3	Adsorption temperature (°C)	20	30	40

2.5. Adsorption Experiments of Methylene Blue and Congo Red onto BCs

The stock solutions of dyes (methylene blue (MB, 100 mg L⁻¹) and congo red (CR, 100 mg L⁻¹) were used for the adsorption study of dyes (MB and CR) onto BCs. The stock solutions of dyes were adjusted to pH 4, 7, and 10 by 1M HCl and 1M NaOH. A 0.01 g of the BCs produced at 350–750 °C was added to 20 mL of MB solution (100 mg L⁻¹) and CR solution (100 mg L⁻¹) in 50 mL glass vials. These experiments were performed in a shaking incubator at various temperatures, such as 20 °C, 30 °C, and 40 °C, with shaking at 200 rpm for 5 days. Then the supernatants were collected to measure the adsorption efficiency after centrifugation of samples at 5000 rpm. The MB and CR value in aqueous phase was measured as an absorbance at 660 nm and 500 nm, respectively. The results were converted to the concentration using the calibration curve (concentration vs. absorbance). The correlations between dye concentration and absorbance were made through regression analysis:

For MB,

$$Y = 4.4818X - 1.2352 \quad (R^2 = 0.9999) \quad (2)$$

For CR,

$$Y = 33.692X + 0.0278 \quad (R^2 = 0.9999) \quad (3)$$

where Y is dye concentration measured, and X is absorbance measured.

The MB adsorption efficiency was calculated following Equation (4):

$$\text{Adsorption efficiency (\%)} = (A - B)/A \times 100 \quad (4)$$

where A is the initial concentration of dye, and B is the final concentration of dye after adsorption experiment.

The MB adsorption capacity was calculated following Equation (5):

$$\text{Adsorption capacity (q)} = \frac{(C_0 - C_i) \times V}{W} \quad (5)$$

where (q): mg of dye adsorbed onto the biochar; (C₀): initial dye concentration in mg per L; [C_i]: final dye concentration in mg per L; V: volume of dye solution in L; W: amount of biochar in g.

2.6. Effect of Adsorption of Dye Mixtures onto BC550

The stock solutions of dyes (i.e., MB (100 mg L⁻¹) and CR (100 mg L⁻¹), and mixtures of MB (100 mg L⁻¹) and CR (100 mg L⁻¹) were prepared to investigate adsorption efficiency at the optimal conditions. Based on the optimization results by RSM, the stock solutions were prepared with pH 7, and 0.01 g of the chosen BC550 was added into 20 mL of each stock solution (i.e., MB, CR solution, and mixtures of MB and CR). The adsorption experiments were conducted at 30 °C (the optimal adsorption temperature from RSM results) and 200 rpm for 5 days.

3. Results and Discussion

3.1. Characterization of Biochar

The physicochemical properties of the BCs produced at three different pyrolysis temperatures (i.e., 350, 550, and 750 °C) have been already discussed in detail in our previous report [9]. In brief, H, O, and N contents decreased with the increase of pyrolysis temperature. C contents also decreased in the current investigation due to the loss of volatile compounds [2]. Nevertheless, O/C and H/C values indicating hydrophobicity and aromaticity decreased with the increase of pyrolysis temperature [9]. In addition, the BET surface area of BCs gradually increased (2–191 m²/g) with higher pyrolysis temperature, indicating cracking of feedstock and development of the pore structures. Similarly, results have also been observed and reported for various BCs [2,10]. The p*H*_{pzc} of BC350, BC550, and BC750 was 6.3, 9.2, and 9.3, respectively. These results imply that BCs have a different surface charge at the

chosen solution pH [10,20]. In addition, it is thought that the higher pH_{pzc} of BC550 and BC750 causes concentrated alkali salts (e.g., Ca, Mg, Na, K, etc.) by the increase of pyrolysis temperature [10,20].

The XRD patterns of BCs were also analyzed and reported in our previous work [9]. The 2-theta diffraction peaks at 15, 24, 26, and 30 for MgCO₃ and 29, 35, 39, 43, 47, and 48 for CaCO₃ were detected [7,9]. BC550 and BC750 showed higher CaCO₃ crystallinity, while BC350 showed higher MgCO₃ crystallinity. These results may imply that CaCO₃ leads to a remarkable dye adsorption. Please see the detailed discussion of adsorption mechanisms in Section 3.4.

3.2. Effects of pH, Pyrolysis Temperature, and Adsorption Temperature on Adsorption Efficiency from RSM Results

In the present study, the different operating conditions including pH (4, 7, and 10), adsorption temperature (20, 30, and 40 °C), and pyrolysis temperature (350, 550, and 750 °C) were evaluated using a Box–Behnken design to study their influence on dye adsorption efficiency. The response (adsorption efficiency, %) is presented as summarized in Table 3. As shown in Figure 1A–F, the two-dimensional (2D) contour plots describe the effect of various variables (pH, adsorption temperature, and pyrolysis temperature) on single dye adsorption efficiency. As shown in Figure 1A,C, the adsorption of MB was facilitated at the high solution pH of 9–10. These results are consistent with previous research using vermicompost-derived BCs and vegetal fiber activated carbons [2,21]. When the solution pH is higher than pH_{pzc} (BCs: 6.3, 9.2, and 9.3), the surface of biochar becomes negatively charged, while it has a positive charge at a pH lower than pH_{pzc}. Therefore, the adsorption of MB could increase owing to the increase in the electrostatic attraction between negatively charged BCs and positively charged MB as a cationic dye at higher pH [17,22,23].

Table 3. Effects of different combinations of various variables on adsorption efficiency (%) of methylene blue and congo red analyzed by using a Box–Behnken response surface design.

Run	Independent Variables			Response (Adsorption Efficiency, %)	
	X1	X2 (°C)	X3 (°C)	Methylene Blue	Congo Red
	pH	Pyrolysis Temperature	Adsorption Temperature	Experimental	Experimental
1	4	350	30	11.38 ± 0.54	52.61 ± 3.37
2	10	350	30	20.54 ± 0.75	15.01 ± 0.01
3	4	750	30	13.84 ± 1.64	98.70 ± 2.40
4	10	750	30	23.88 ± 4.40	23.27 ± 1.79
5	4	550	20	10.04 ± 0.06	16.19 ± 1.14
6	10	550	20	16.96 ± 8.43	14.84 ± 1.18
7	4	550	40	25.45 ± 0.78	98.75 ± 0.35
8	10	550	40	45.09 ± 4.11	97.79 ± 0.29
9	7	350	20	4.46 ± 2.07	4.38 ± 0.87
10	7	750	20	10.04 ± 0.06	16.36 ± 2.32
11	7	350	40	14.29 ± 1.81	6.24 ± 0.33
12	7	750	40	39.06 ± 1.32	98.87 ± 1.23
13	7	550	30	20.98 ± 0.02	97.99 ± 1.40
14	7	550	30	33.48 ± 0.73	97.77 ± 0.31
15	7	550	30	20.31 ± 3.80	97.99 ± 1.40

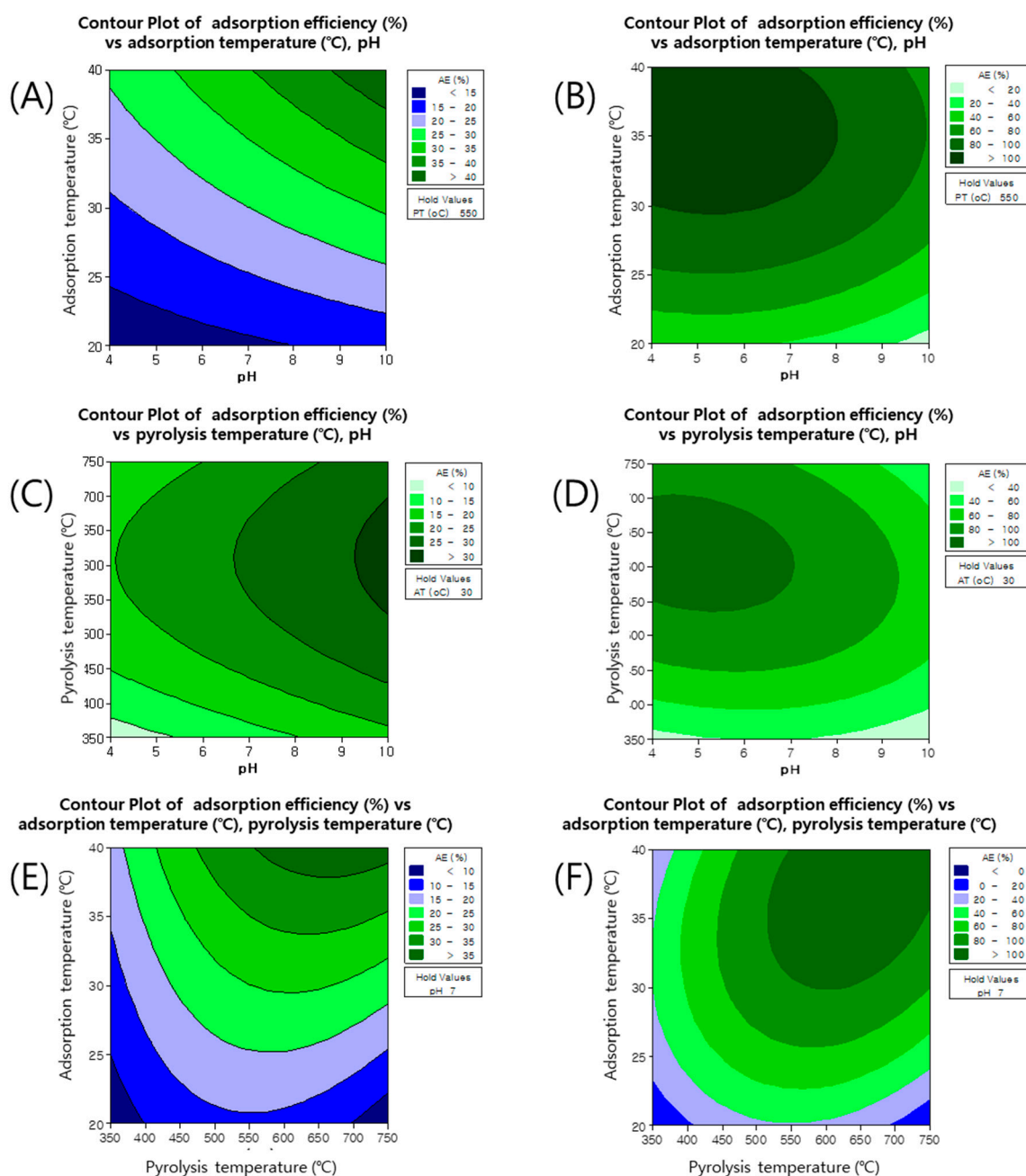


Figure 1. Two-dimensional contour plots showing effects of pH, pyrolysis temperature (PT, °C), and adsorption temperature (AT, °C) on adsorption efficiency of methylene blue (MB) (A,C, E) and congo red (CR) (B,D,F).

These results were similar to the phenomena (the CR adsorption onto vermicompost-derived BCs) from the previous literature, but there was no effect of solution pH on the CR adsorption by rice straw, wood chip, and Korean cabbage-derived BCs [2,4].

In addition, the increase of adsorption temperature and pyrolysis temperature influenced the adsorption efficiency of both dyes (MB and CR) as shown in Figure 1E,F. At solution pH 7, the best operating conditions were between 550 to 750 °C of the pyrolysis temperature and between 35 to 40 °C of adsorption temperature for the adsorption efficiency (80%–100%) of MB and CR. According to a previous study, the MB adsorption by anaerobic digestion residue and eucalyptus-derived BCs was enhanced with the increase of the reaction temperature [7]. These results imply that the BCs produced

at higher temperature can be potential adsorbents, and the dyes' adsorption can be associated with a spontaneous reaction.

3.3. Effects of Single Dye and Dye Mixtures on Adsorption Efficiency at the Chosen Conditions

Predicted values of various variables for optimum adsorption efficiency of MB and CR presented in Figure 2. In the case of MB, pH 9.4, pyrolysis temperature 673 °C, and 40 °C of adsorption temperature were predicted as the best conditions for MB adsorption, implying 45% of adsorption efficiency and 90 mg MB/g BC of adsorption capacity (Figure 2A).

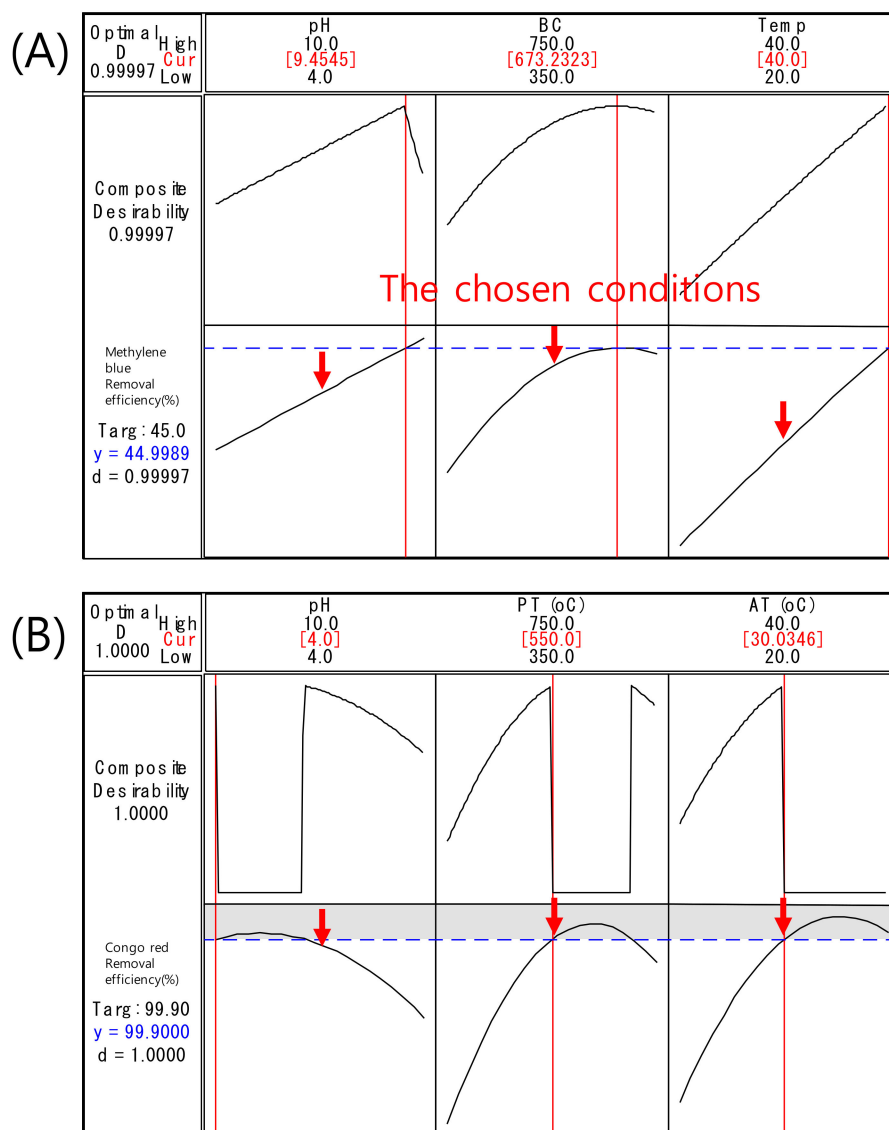


Figure 2. Predicted values of different variables (pH, pyrolysis temperature (PT, °C), and adsorption temperature (AT, °C)) for optimum adsorption efficiency. (A): MB, (B): CR. Symbol (↓) is the chosen conditions for the adsorption of mixtures of MB and CR.

In contrast, Figure 1B,D shows the influence of solution pH between the adsorption of CR and biochar. The adsorption of CR was higher at lower pH, indicating the BCs are protonated when the solution pH (4–6) is lower than the pH_{pzc} of the BCs (6.3, 9.2, and 9.3). The electrostatic attraction between the positively charged BCs and the negatively charged CR as an anionic dye will be strengthened with pH decrease, resulting in the increase of CR adsorption.

The MB adsorption capacity of maple-derived BCs used in this investigation was higher than that of anaerobic digestion residue-derived BCs (9.5 mg MB/g BC), sewage and tea waste-derived BCs (12.5 mg MB/g BC), pulp and paper sludge-derived BCs (33 mg MB/g BC), and sewage sludge-derived BCs (14–45 mg MB/g BC) but lower than that of vermicompost-derived BCs (174 mg MB/g BC), orange peel (526 mg/g BC), and banana biomass (426 mg/g BC) BCs [2,7,17,24,25]. These results indicate that the maple-derived BCs possessed significant ability (e.g., functional groups, metals, and electrostatic attraction) with regard to MB adsorption.

As shown in Figure 2B, the CR adsorption of maple-derived BCs was great at pH 4, 550 °C of pyrolysis temperature, and 30 °C of adsorption temperature. At these conditions, the CR adsorption efficiency and capacity were 99% and 198 mg CR/g BC, respectively.

According to previous studies, the CR adsorption capacity by rice straw, vermicompost, wood chip-derived BCs was 190, 31, and 110 mg CR/g BC, respectively, and for activated carbon it was 769 mg CR/g BC [2,4]. The CR adsorption mechanisms by these BCs often contained electrostatic interaction and oxygen-containing functional groups, indicating the chemical sorption between BCs and CR [2].

The chosen conditions (i.e., solution pH 7, 30 °C of adsorption temperature, and 550 °C of pyrolysis temperature) were selected to evaluate the effect of single dye and dye mixture on adsorption efficiency according to the RSM results (Figure 3). In particular, among them, the initial pH of the dye solution was set at pH 7 to avoid the additional use of chemicals for the adjustment of pH and to reduce the bias to acid and base. Moreover, the adsorption and pyrolysis temperatures were chosen for the experiment, taking into account the cost. At these chosen conditions, the adsorption efficiencies of both MB and CR by single reaction were 25% (adsorption capacity: 49 mg MB/g BC) and 97% (adsorption capacity: 195 mg CR/g BC), respectively, as shown in Figure 3. On the other hand, the adsorption efficiency for each dye in a dye mixture reaction appeared as 68% for MB and 74% for CR, indicating the increase of MB adsorption efficiency and the decrease of CR adsorption efficiency compared to those of a single reaction. These results suggest that the competition and the reaction time for the adsorption of each dye on the active sites of the BC surface may be possible causes, although it could not be fully understood. Based on these finding, this biochar-based adsorptive approach for the treatment of dye mixtures can be applied, depending on the characteristics of dye wastewater such as pH, initial concentration of each dye, and sorts of dye. Furthermore, the evaluation using RSM can be rapidly and effectively conducted for the adsorption of the dye mixture.

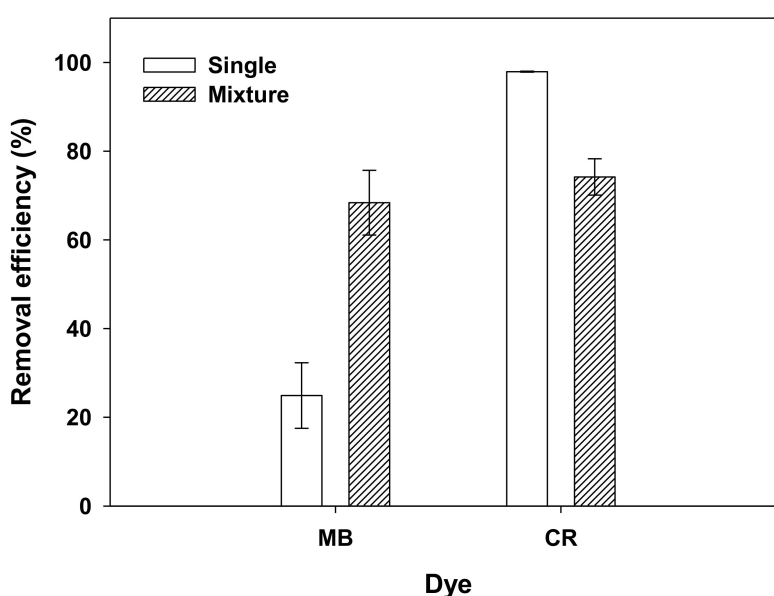


Figure 3. Comparison of adsorption in single dye (methylene blue (MB) or congo red (CR)) and dye mixture (MB and CR) dye solutions onto BC 550 at 30 °C and pH 7.

3.4. Possible Mechanisms for Dye Adsorption onto BC550

The FTIR spectra of the BC550 surface before and after the adsorption of single dye and dye mixtures are shown in Figure 4. After the dye adsorption, the FTIR spectrum of BC550 confirmed the absence of various bands such as carbonates (CO_3^{2-} , 875 cm^{-1}), C-O stretching (1049 cm^{-1}), and C-H (1430 cm^{-1}). As reported in the previous literature, these functional groups may participate in MB sorption [22]. Therefore, it was obvious that BC550 comprises binding sites for the dye adsorption. In addition, a significant increase of peaks at 1036 cm^{-1} and 1640 cm^{-1} under the adsorption of dye mixtures emerged, compared to those under the adsorption of a single dye. These results imply that MB and CR were simultaneously adsorbed onto BC550.

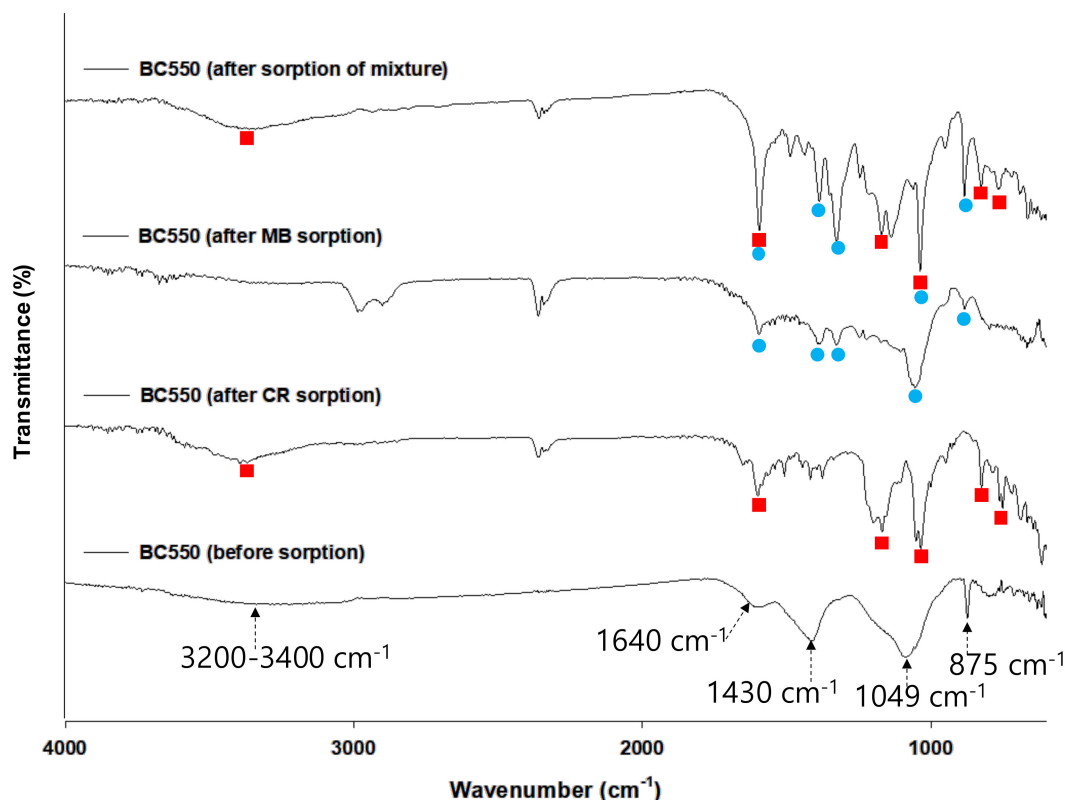


Figure 4. Fourier transform infrared (FTIR) spectra of BC550 before and after sorption of single dye and dye mixtures.

XPS results of the BC550 and dye-bound BC550 were compared to determine the detailed binding matrix related to the adsorption of a single dye and dye mixture by BCs (Figure 5A–F). C1s, Ca2p, N1s, O1s, and Mg1s were visible in the survey scan of BC550. The O1s and Mg1s were associated with the CR adsorption, whereas C1s, Ca2p, O1s, and Mg1s were associated with the MB adsorption (Figure 5A). As shown in Figure 5B, the decrease of functional groups (C–H) mainly appeared during MB adsorption [26]. As mentioned in Section 3.1, it was demonstrated that the dye adsorption was induced by the decrease of Ca^{2+} and Mg^{+} ions (Figure 5D,E).

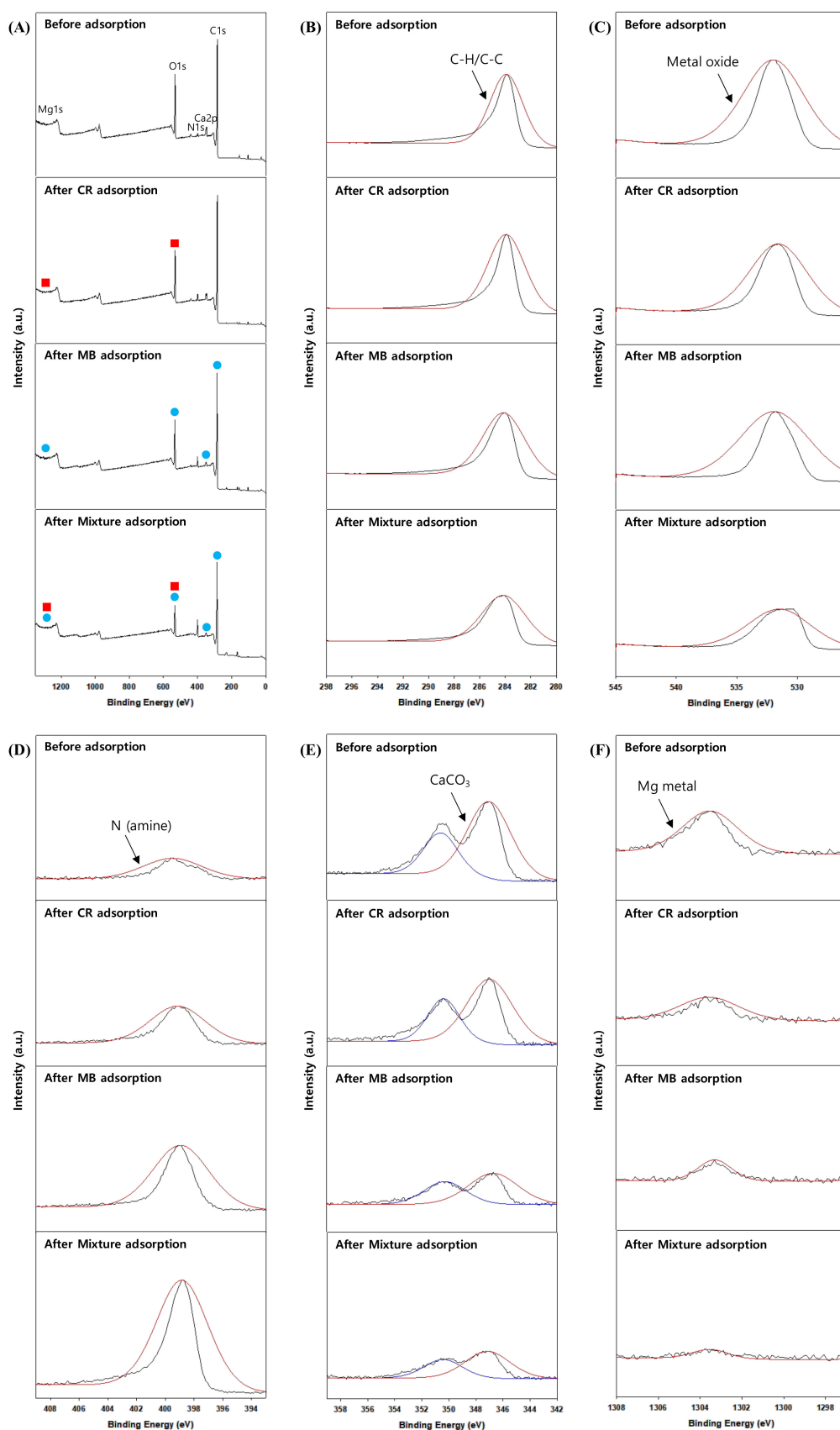


Figure 5. XPS of (A) survey scan, (B) C1s, (C) O1s, (D) N1s, (E) Ca2p, and (F) Mg1s of BC550 before and after adsorption reaction.

As reported in a previous study, the MB and CR adsorption may be assigned by ion exchange processes, such as of Ca^{2+} and Mg^{+} ion [2,22]. In contrast, the increase of N1s could be related to N source in MB and CR after the adsorption. These results indicate C1s, O1s, Ca2p, and Mg1s as binding sites, indicating functional group and ion exchange influenced the dye adsorption. Thus, maple leaf-derived BCs can be applied for cationic and anionic dye elimination as a low-cost and effective adsorbent.

4. Conclusions

In this work, maple leaf BCs produced at different pyrolysis temperatures were investigated for the removal of dye, i.e., methylene blue and congo red. Biochar MB550 was observed as an efficient adsorbent for the removal of both dyes from mixtures. Pyrolysis temperature, pH, and temperature of reaction were observed as important factors for selectivity and adsorption efficiency of dyes. Experimental results under selected conditions showed that MB550 was able to remove MB and CR from dye mixtures with 68% and 74% efficiency. Future plans are needed to investigate the correlation between the chemicals, and other pollutants contained in dye effluent, and the adsorption efficiency onto BCs. In addition, a more detailed dye adsorption study using real wastewater is required.

Author Contributions: Y.-K.C.; Conceptualization, methodology, formal analysis, writing—original draft preparation, R.G.; resources, data curation, H.J.K.; writing—review and editing, supervision, Y.-H.Y.; validation, visualization, S.K.B.; Conceptualization, writing—original draft preparation, supervision. All authors have read and agreed to the published version of the manuscript.

Funding: This research was supported by Basic Science Research Program through the National Research Foundation of Korea (NRF) funded by the Ministry of Education (NRF-2019R1I1A1A01054638, NRF-2015M1A5A1037196, NRF-2019M3E6A1103979, 2017R1D1A1B03030766). The authors would also like to acknowledge the KU Research Professor Program of Konkuk University, Seoul, South Korea.

Conflicts of Interest: The authors declare no conflict of interest.

References

1. Chen, H.; Zhao, J. Adsorption study for removal of Congo red anionic dye using organo-attapulgit. *Adsorption* **2009**, *15*, 381–389. [[CrossRef](#)]
2. Yang, G.; Wu, L.; Xian, Q.; Shen, F.; Wu, J.; Zhang, Y. Removal of congo red and methylene blue from aqueous solutions by vermicompost-derived biochars. *PLoS ONE* **2016**, *11*, e0154562. [[CrossRef](#)]
3. Katheresan, V.; Kansedo, J.; Lau, S.Y. Efficiency of various recent wastewater dye removal methods: A review. *J. Environ. Chem Eng.* **2018**, *6*, 4676–4697. [[CrossRef](#)]
4. Sewu, D.D.; Boakye, P.; Woo, S.H. Highly efficient adsorption of cationic dye by biochar produced with Korean cabbage waste. *Bioresour. Technol.* **2017**, *224*, 206–213. [[CrossRef](#)] [[PubMed](#)]
5. Paz, C.B.; Araújo, R.S.; Oton, L.F.; Oliveira, A.C.; Soares, J.M.; Medeiros, S.N.; Rodríguez-Castellón, E.; Rodríguez-Aguado, E. Acid Red 66 dye removal from aqueous solution by Fe/C-based composites: Adsorption, kinetics and thermodynamic studies. *Materials* **2020**, *13*, 1107. [[CrossRef](#)] [[PubMed](#)]
6. Khedher, M.; Mossad, M.; El-Etriby, H.K. Enhancement of electrocoagulation process for dye removal using powdered residuals from water purification plants (PRWPP). *Water Air Soil Pollut.* **2017**, *228*, 293. [[CrossRef](#)]
7. Sun, L.; Wan, S.; Luo, W. Biochars prepared from anaerobic digestion residue, palm bark, and eucalyptus for adsorption of cationic methylene blue dye: Characterization, equilibrium, and kinetic studies. *Bioresour. Technol.* **2013**, *140*, 406–413. [[CrossRef](#)]
8. Ahmed, M.; Okoye, P.; Hummadi, E.; Hameed, B. High-performance porous biochar from the pyrolysis of natural and renewable seaweed (*Gelidiella acerosa*) and its application for the adsorption of methylene blue. *Bioresour. Technol.* **2019**, *278*, 159–164. [[CrossRef](#)]
9. Kim, J.E.; Bhatia, S.K.; Song, H.J.; Yoo, E.; Jeon, H.J.; Yoon, J.-Y.; Yang, Y.; Gurav, R.; Yang, Y.-H.; Kim, H.J. Adsorptive removal of tetracycline from aqueous solution by maple leaf-derived biochar. *Bioresour. Technol.* **2020**, 123092. [[CrossRef](#)]

10. Choi, Y.-K.; Choi, T.-R.; Gurav, R.; Bhatia, S.K.; Park, Y.-L.; Kim, H.J.; Kan, E.; Yang, Y.-H. Adsorption behavior of tetracycline onto *Spirulina* sp.(microalgae)-derived biochars produced at different temperatures. *Sci. Total Environ.* **2020**, *710*, 136282. [[CrossRef](#)]
11. Kharel, G.; Sacko, O.; Feng, X.; Morris, J.R.; Phillips, C.L.; Trippe, K.; Kumar, S.; Lee, J.W. Biochar surface oxygenation by ozonization for super high cation exchange capacity. *ACS Sustain. Chem. Eng.* **2019**, *7*, 16410–16418. [[CrossRef](#)]
12. Huff, M.D.; Marshall, S.; Saeed, H.A.; Lee, J.W. Surface oxygenation of biochar through ozonization for dramatically enhancing cation exchange capacity. *Bioresour. Bioprocess.* **2018**, *5*, 18. [[CrossRef](#)]
13. Somsesta, N.; Sricharoenchaikul, V.; Aht-Ong, D. Adsorption removal of methylene blue onto activated carbon/cellulose biocomposite films: Equilibrium and kinetic studies. *Mater. Chem. Phys.* **2020**, *240*, 122221. [[CrossRef](#)]
14. Bhatia, S.K.; Gurav, R.; Choi, T.-R.; Kim, H.J.; Yang, S.-Y.; Song, H.-S.; Park, J.Y.; Park, Y.-L.; Han, Y.-H.; Choi, Y.-K.; et al. Conversion of waste cooking oil into biodiesel using heterogenous catalyst derived from cork biochar. *Bioresour. Technol.* **2020**, *302*, 122872. [[CrossRef](#)]
15. Gurav, R.; Bhatia, S.K.; Choi, T.-R.; Park, Y.-L.; Park, J.Y.; Han, Y.-H.; Vyavahare, G.; Jadhav, J.; Song, H.-S.; Yang, P.; et al. Treatment of furazolidone contaminated water using banana pseudostem biochar engineered with facile synthesized magnetic nanocomposites. *Bioresour. Technol.* **2020**, *297*, 122472. [[CrossRef](#)]
16. Li, G.; Zhu, W.; Zhang, C.; Zhang, S.; Liu, L.; Zhu, L.; Zhao, W. Effect of a magnetic field on the adsorptive removal of methylene blue onto wheat straw biochar. *Bioresour. Technol.* **2016**, *206*, 16–22. [[CrossRef](#)]
17. Chaukura, N.; Murimba, E.C.; Gwenzi, W. Sorptive removal of methylene blue from simulated wastewater using biochars derived from pulp and paper sludge. *Environ. Technol. Inno.* **2017**, *8*, 132–140. [[CrossRef](#)]
18. Ayari, F.; Khelifi, S.; Othman, A.B.; Ayadi, M.T. Case studies focusing on the most successful advanced methods/approach for the treatment of nanomaterials in wastewater. In *Emerging and Nanomaterial Contaminants in Wastewater*; Elsevier: Amsterdam, The Netherlands, 2019; pp. 311–353. [[CrossRef](#)]
19. Choi, Y.-K.; Kan, E. Effects of pyrolysis temperature on the physicochemical properties of alfalfa-derived biochar for the adsorption of bisphenol A and sulfamethoxazole in water. *Chemosphere* **2019**, *218*, 741–748. [[CrossRef](#)]
20. Usman, A.R.; Abduljabbar, A.; Vithanage, M.; Ok, Y.S.; Ahmad, M.; Ahmad, M.; Elfaki, J.; Abdulazeem, S.S.; Al-Wabel, M.I. Biochar production from date palm waste: Charring temperature induced changes in composition and surface chemistry. *J. Anal. Appl. Pyrol.* **2015**, *115*, 392–400. [[CrossRef](#)]
21. Cherifi, H.; Fatiha, B.; Salah, H. Kinetic studies on the adsorption of methylene blue onto vegetal fiber activated carbons. *Appl. Surf. Sci.* **2013**, *282*, 52–59. [[CrossRef](#)]
22. Fan, S.; Tang, J.; Wang, Y.; Li, H.; Zhang, H.; Tang, J.; Wang, Z.; Li, X. Biochar prepared from co-pyrolysis of municipal sewage sludge and tea waste for the adsorption of methylene blue from aqueous solutions: Kinetics, isotherm, thermodynamic and mechanism. *J. Mole Liq.* **2016**, *220*, 432–441. [[CrossRef](#)]
23. Lyu, H.; Gao, B.; He, F.; Zimmerman, A.R.; Ding, C.; Tang, J.; Crittenden, J.C. Experimental and modeling investigations of ball-milled biochar for the removal of aqueous methylene blue. *Chem. Eng. J.* **2018**, *335*, 110–119. [[CrossRef](#)]
24. Leng, L.; Yuan, X.; Huang, H.; Shao, J.; Wang, H.; Chen, X.; Zeng, G. Bio-char derived from sewage sludge by liquefaction: Characterization and application for dye adsorption. *Appl. Surf. Sci.* **2015**, *346*, 223–231. [[CrossRef](#)]
25. Amin, M.T.; Alazba, A.A.; Shafiq, M. Comparative study for adsorption of methylene blue dye on biochar derived from orange peel and banana biomass in aqueous solutions. *Environ. Monit. Assess.* **2019**, *191*, 735. [[CrossRef](#)] [[PubMed](#)]
26. David, N.; Anavi, D.; Milanovich, M.; Popowski, Y.; Frid, L.; Amir, E. Preparation and properties of electro-conductive fabrics based on polypyrrole: Covalent vs. non-covalent attachment. In *Proceedings of the IOP Conference Series: Materials Science and Engineering*, Corfu, Greece, 29–31 May 2017; p. 032002. [[CrossRef](#)]

